A Case Study in Predictive Three-Dimensional Topography Simulation Based on a Level-Set Algorithm

Clemens Heitzinger[1], Alireza Sheikholeslami[1], Josef Fugger[2], Oliver Häberlen[2], Markus Leicht[2], and Siegfried Selberherr[1]

[1] Institute for Microelectronics
Technical University of Vienna, Austria
Gusshausstrasse 27–29/E360
A-1040 Vienna
Austria
Phone: +43(1)58801–36035
Fax: +43(1)58801–36099
Email: Heitzinger@iue.tuwien.ac.at

[2] Infineon Technologies
Siemensstrasse 2
A-9500 Villach
Austria

A Case Study in Predictive Three-Dimensional Topography Simulation Based on a Level-Set Algorithm

Clemens Heitzinger[1], Alireza Sheikholeslami[1], Josef Fugger[2], Oliver Häberlen[2], Markus Leicht[2], and Siegfried Selberherr[1]

Abstract

The aim of this work is to study the etching of trenches in silicon and the generation of voids during the filling of genuinely three-dimensional trench structures with silicon dioxide or nitride. The trenches studied are part of the manufacturing process of power MOSFETs, where void-less filling must be achieved. Another area of applications is capacitance extraction in interconnect structures, where the deliberate inclusion of voids serves the purpose of reducing overall capacitance. Furthermore, these simulations make it possible to analyze the variations on the feature scale depending on the position of the single trench on the wafer and in the reactor.

Keywords: Feature scale topography simulation, deposition, etching, level set method.

1 Introduction

The deposition of thin layers and the etching of trenches are fundamental for the production of memory cells, power MOSFETs, and backend stacks. For the purposes of feature scale topography simulation, there are three basic geometric operations: deposition of layers, etching of trenches, and CMP (chemical mechanical planarization) which is a straightforward operation on the feature scale level.

The three-dimensional deposition and etching simulations were performed using the topography simulator ELSA (Enhanced Level Set Applications) which is based on a level set algorithm for describing moving boundaries. It includes narrow banding and a fast marching algorithm for the suitable extension of the speed function [9, 21]. The particle trajectories in the simulation domain are tracked via an iterative radiosity formulation. The dominating reactions paths are based on the main reacting species [19]. The ion angular distribution function (IADF) entering the simulation domain and the location of the ion sources are determined by the plasma and this information enters the feature scale simulation as physical boundary condition. The ions at the wafer surface are reflected in a specular manner in addition to a cosine law around the angle of the reflection.

Despite the magnitude of computational resources available today, care must be taken in the choice of algorithms to achieve sensible computing times for three-dimensional simulations. The optimized level set algorithm for describing the moving boundaries is presented in Section 2. The increase in computation time when the spatial resolution is increased is investigated in Section 2.3. In Section 3 the physical models of the transport of the particles, for film growth, and for etching the substrate are discussed.

Finally in Section 4 examples stemming from the etching and filling of trenches with silicon dioxide or nitride for manufacturing power devices are presented. The filling of T- and H-shaped trench junctions requires truly three-dimensional simulations.

2 Representation of Surfaces

An early approach to describing the time evolution of boundaries was the string method. The string algorithm was proposed in [13] and is based on the straightforward idea to approximate the boundary considered by line segments forming a string in two spatial dimensions and by a triangular surface mesh in three dimensions. Depending on the local speed the points are moved along the bisectors of the angles between two neighboring line segments.

During the movement of the surface, the density of the points has to kept roughly uniform by inserting points where the surface expands and

by deleting them where the surface shrinks. The formation of superfluous loops and self-intersections, however, causes problems especially when the speed of the movement of the boundary strongly varies [24]. This problem is inherent to the string algorithm. The loops are small in the beginning, but they expand as the simulation continues and can even intersect one another.

In the cellular approach the simulation domain is divided into a homogeneous array of cuboid cells. An early implementation of a cellular approach was presented in [5]. For moving the surface two possibilities are known: the cell removal algorithm and the structuring element algorithm.

The cell removal algorithm simply removes cells near the surface depending on the amount of etching taking place. In addition to performance problems faceting takes place which poses a serious problem. Faceting means that, e.g., an octagon instead of a circle occurs when uniform isotropic etching starting at a single seed point is simulated [13]. This is inherent to the cell removal algorithm and prompted the development of various sophisticated methods.

The structuring element algorithm is a remedy to the faceting problem and works by moving a structuring element along the surface. The shape and size of the structuring element depends on the process modeled and the local etching and deposition rate. This idea stems from digital image processing, where it is well-known [7].

The advantages of the cellular approach to surface description are its robustness and ease of implementation. One problem is that the resolution is limited by the size of the surface elements and hence representing slightly tilted surfaces requires high resolutions. Furthermore the precise calculation of surface normals is impossible, although a good solution was achieved in [17].

In recent years the level set method has received lots of attention in TCAD simulations and in fluid dynamics. It is the newest of the three methods and its basic idea is to represent the surface in question as the set of all zeroes of a certain function, i.e., as its zero level set. Its impact is underlined by the several implementations that have been reported in the realm of TCAD [1, 2, 9, 10, 12, 21].

The level set method is not only used in TCAD, but it has also been proposed as a means of tracking moving boundaries in other areas like computational geometry, image enhancement and noise removal, shape detection and recognition, electromigration, and grid generation [20].

The main advantages of the level set method are the relatively fine resolution that can be achieved, the handling of slightly tilted lines and corners, and the precise and easy calculation of surface normals. Furthermore joining surfaces is handled implicitly by the algorithm. On the other hand, efficient level set algorithms that work stably and accurately for many time steps are more complicated than the cellular approach.

In order to arrive at a practical level set algorithm in three spatial dimensions, care must be taken when choosing data structures and the single algorithms acting on them. These issues and the path taken in this work are discussed in the following.

2.1 Initialization

In the first step the level set function must be initialized to the signed distance function. Since the level set algorithm will later work only in the narrow band, it is sufficient to perform the distance calculations near the initial boundary. This can be achieved, e.g., by a recursive algorithm walking along the boundary. First, a point whose distance to the boundary is smaller than the width of the future narrow band is found by walking along the boundary of the simulation domain parallel to the trench. When such a point is found, it is used as the starting point for the recursion. In the recursion, only points with distance lower than the narrow band width are considered for the next step. The maximum distance ever computed during this procedure is used for initializing the grid points above and below the boundary with positive resp. negative sign. The distance of a point from a triangle t is given by $d(P,t) = \min_{T \in t} \|P - T\|_2$ and the distance $d(P,b)$ of a point from the initial boundary $b = \{t_1, \ldots, t_m\}$, consisting of a set of triangles, is given by $d(P,b) = \min_{t \in b} d(P,t)$.

This method reduces the computational effort of initialization from $O(n^3)$ to $O(n^2)$, where n is the number of grid points in each direction and where it is assumed that the boundary has the shape customarily considered in semiconductor process simulation.

Starting from an initial boundary consisting of about twenty triangles and using a narrow band width of three times the grid spacing on both sides of the boundary, the initialization step for a 100^3 grid takes less than 10 seconds on a Pentium IV class personal computer. A fast marching method is of the same computational effort of $O(n^2)$.

2.2 Narrow Banding and Extending the Speed Function

Combining narrow banding and extending the speed function was described in [11]. The benefit of this algorithm is that it renders reinitialization superfluous. Frequent reinitialization which would be necessary otherwise is generally considered critical since it introduces inaccuracies [22]. Ensuring that the level set function remains the signed distance function throughout simulations also facilitates joining different deposition and etching steps, since the level set grid values can be reused.

2.3 Discretization and Computational Complexity

A second order space convex finite difference scheme [4,8,15,16] was used for the simulations in Section 4.

The spatial and temporal discretization steps Δx, Δy, Δz, and Δt are connected via a Courant–Friedrichs–Levy (CFL) condition which demands that the front must not cross more than one grid cell in each time step and ensures the stability of the scheme. The CFL condition is an information theoretic one and it is fundamental in the sense that it is not affected by the choice of the numeric method, be it finite differences or finite elements, etc.

The CFL condition requires that

$$\Delta t \max_{\text{domain}(F)} F \leq \min(\Delta x, \Delta y, \Delta z).$$

Assuming that $\max F$ remains constant as the spatial resolution is increased, a finer grid necessitates an increase in the number of time steps. Furthermore, considering the realistic case that the overall real time span of the simulation is given, increasing the spatial resolution by a factor λ, the number of time step increases by λ as well. In each time step the number of extracted surface elements increases by λ^2 and thus the effort for the visibility test by λ^4. In summary, an increase of the spatial resolution by λ causes an increase in simulation time by λ^5 due to the CFL condition for numeric stability. This relationship is fundamental to simulations where the boundary is moved by a level set method irrespective of the numeric method.

The increase in simulation time is illustrated by the timing results given in Table 2.

2.4 Boundary and Void Extraction

The code for boundary and void extraction on cuboid grids is not as straightforward as in two dimensions. Although the basic idea is clear, the combinations of the signs of the vertices of the cuboids lead to a non-trivial case differentiation. An in-depth discussion of these issues can be found in [14].

In order to make topography simulations part of a simulation flow including, e.g., implantation, diffusion, or capacitance extractions, it is necessary to translate triangulated surfaces to volume meshes and vice versa. In order to initialize the level set grid from a surface consisting of a large number of small triangles, it is advantageous to use a fast marching algorithm (cf. Section 2.2). In order to construct volume meshes from extracted boundaries, the grid generator DELINK [6] can be used.

3 Transport and Surface Reaction Models

In this section we summarize how the transport of particles in the boundary layer above the wafer and how the surface reactions are handled. For

most of today's processes the Knudsen number is small and hence transport happens in the radiosity regime.

3.1 Visibility Test

The visibility test is the most computationally expensive part of feature scale topography simulation and hence great care must be taken to ensure it works efficiently. Its computational effort grows like $O(m^2)$, where m is the number of surface elements, and this number grows like $O(n^2)$, where n is the number of grid points in each direction.

Two surface elements are visible from one another, if the connecting line between their centers of mass does not intersect the boundary, i.e., the zero level set. Since after initialization – if performed as described in Section 2.1 – the values of the level set grid are a lower bound for the distance of each point to the boundary, it is not necessary to consider every grid cell while walking along the connecting line in the far away region, i.e., not in the narrow band. Of course the actual time consuming calculations of detecting changes of sign must be performed only in the narrow band.

This means that there is a trade-off between the width of the narrow band and the time consumed by the visibility test. The smaller the narrow band, the less information is known about the distance to the boundary and thus the step size, while walking along the connecting line between the two surface elements, is smaller than for a wider narrow band.

In order to speed up the visibility test further while sacrificing accuracy, it may be beneficial to define that two triangles are visible from one another if the middle points of the grid cell in which they are located do not intersect the boundary. Since each grid cell contains at least two triangles, this simplification leads to considerable time saving.

3.2 Radiosity

The cases of etching and deposition must be handled differently in radiosity simulations. This is outlined in Table 1.

3.3 Deposition

Three models for the TEOS deposition reaction have been proposed: a heterogeneous deposition model, a homogeneous intermediate-mediated deposition model and a heterogeneous deposition with byproduct inhibition model. These are discussed, e.g., in [18] where it is concluded that TEOS pyrolysis likely occurs through the heterogeneous deposition mechanism in which TEOS decomposition products readsorb on the growing film and inhibit deposition.

For the purposes of the deposition of silicon nitride films, we use

$$SiH_4 + NH_3 \rightarrow SiNH + 3H_2$$

as the essential reaction. A detailed model of triaminosilane condensation can be found in [23].

3.4 Etching

The ion angular distribution function (IADF) entering the simulation domain and the location of the ion sources are determined by the plasma and this information enters the feature scale simulation as physical boundary condition. The ions at the wafer surface are reflected in a specular manner in addition to a cosine law around the angle of the reflection.

For chlorine etching we have

$$\begin{aligned} {Cl^+}_{(g)} + S &\rightarrow Cl_{(s)} \\ Si_{(s)} + 4Cl_{(s)} &\rightarrow SiCl_{4(g)} + 4S, \end{aligned}$$

where S denotes a surface site, as the dominating reaction path [3, 19].

4 Simulation Results

In some cases, e.g. cylindrical structures, the special symmetry of the problem can be exploited to reduce three-dimensional simulation problems to those that can be handled by two-dimensional geometry descriptions and special summation formulas.

Here the applications, namely trenches with T- and H-junctions, are genuinely three-dimensional geometries and show three-dimensional effects as will be seen in the etching results. The example stems from the etching of trench structures with several junctions and their filling by silicon dioxide. These manufacturing steps occur during the production of power MOSFETs.

Figure 1 shows an isotropic etching process and Figure 2 shows the result of directional etching using chlorine, where the incoming flux is not perpendicular to the wafer surface. Figure 3 shows the deposition of silicon dioxide into a cylindrical trench, where a void is formed. Figure 4 shows the initial geometry of an H-shaped trench and Figure 5 the deposited layer.

The simulation times for a 30^3 and a 60^3 grid on a Pentium IV computer running at 2.8GHz are shown in Table 2. A whole simulation typically consists of 100 or 200 steps.

[Table 1 about here.]

[Table 2 about here.]

[Figure 1 about here.]

[Figure 2 about here.]

[Figure 3 about here.]

[Figure 4 about here.]

[Figure 5 about here.]

5 Conclusion

The three-dimensional simulator is used during the development of the topography manufacturing steps of power MOSFETs for automotive applications. The simulator was found to be applicable to a wide range of both etching and deposition problems and to yield predictive simulations within a reasonable time frame. Furthermore the trade-offs for an efficient three-dimensional simulator based on the level set method were discussed.

References

[B0408]

[1] D. Adalsteinsson and J.A. Sethian. A level set approach to a unified model for etching, deposition, and lithography iii: Re-deposition, re-emission, surface diffusion, and complex simulations. Technical report, Department of Mathematics and Lawrence Berkeley Laboratory, University of California, Berkeley, California 94720, August 1997.

[B0409]

[2] T.J. Barth and J.A. Sethian. Numerical schemes for the hamilton-jacobi and level set equations on triangulated domains. Technical report, Information Sciences Directorate, NASA Ames Research Center and Department of Mathematics, University of California, Berkeley, September 1997.

[chang1998plasma]

[3] J.P. Chang, A.P. Mahorowala, and H.H. Sawin. Plasma-surface kinetics and feature profile evolution in chlorine etching of polysilicon. *J. Vac. Sci. Technol. A*, 16(1):217–224, 1998.

[crandall1983viscosity]

[4] M.G. Crandall and P.-L. Lions. Viscosity solutions of Hamilton–Jacobi equations. *Trans. Amer. Math. Soc.*, 277:1–42, 1983.

[P0613]

[5] F.H. Dill, A.R. Neureuther, J.A. Tuttle, and E.J. Walker. Modeling projection printing of positive photoresists. *IEEE Trans. Electron Devices*, ED-22(7):456–464, 1975.

[B0447]

[6] P. Fleischmann. *Mesh Generation for Technology CAD in Three Dimensions*. Dissertation, Technische Universität Wien, 2000. http://www.iue.tuwien.ac.at/phd/fleischmann.

[giardina1988]

[7] C.R. Giardina and E.R. Dougherty. *Morphological Methods in Image and Signal Processing*. Prentice-Hall, New Jersey, 1988.

[harten1987uniformlyIII]

[8] A. Harten, B. Engquist, S. Osher, and S. Chakravarthy. Uniformly high order accurate essentially non-oscillatory schemes. III. *J. Comput. Phys.*, 71(2):231–303, 1987.

[heitzinger2002increasing]

[9] C. Heitzinger, J. Fugger, O. Häberlen, and S. Selberherr. On increasing the accuracy of simulations of deposition and etching processes using radiosity and the level set method. In G. Baccarani, E. Gnani, and M. Rudan, editors, *Proc. 32th European Solid-State Device Research Conference (ESSDERC 2002)*, pages 347–350, Florence, Italy, 2002.

[heitzinger2002inverse]

[10] C. Heitzinger, J. Fugger, O. Häberlen, and S. Selberherr. Simulation and inverse modeling of TEOS deposition processes using a fast level set method. In *Proc. Simulation of Semiconductor Processes and Devices (SISPAD 2002)*, pages 191–194, Kobe, Japan, 2002.

[heitzinger2003predictive]

[11] Clemens Heitzinger, Alireza Sheikholeslami, Helmut Puchner, and Siegfried Selberherr. Predictive simulation of void formation during the deposition of silicon nitride and silicon dioxide films. In R.E. Sah, M.J. Deen, D. Landheer, K.B. Sundaram, W.D. Brown, and D. Misra, editors, *Proc. 203rd Meeting of the Electrochemical Society (ECS), Silicon Nitride and Silicon Dioxide Thin Insulating Films VII*, pages 356–365, Paris, France, 2003.

[P0534]

[12] Z.-K. Hsiau, E.C. Kan, J.P. McVittie, and R.W. Dutton. Robust, stable, and accurate boundary movement for physical etching and deposition simulation. *IEEE Trans. Electron Devices*, 44(9):1375–1385, September 1997.

[jewett1977]

[13] R. Jewett, P. Hagouel, A. Neureuther, and T. van Duzer. Line-profile resist development simulation techniques. *Polymer Engineering and Science*, 17:381–384, 1977.

[nielson2003marching]

[14] G. Nielson. On marching cubes. *IEEE Trans. Visualization and Computer Graphics*, 9(3):283–297, 2003.

[osher1988fronts]

[15] S. Osher and J.A. Sethian. Fronts propagating with curvature-dependent speed: Algorithms based on Hamilton–Jacobi formulations. *J. Comput. Phys.*, 79(1):12–49, 1988.

[osher1991high]

[16] S. Osher and C. Shu. High-order essentially nonoscillatory schemes for Hamilton–Jacobi equations. *SIAM J. Numer. Anal.*, 28(4):907–922, 1991.

[B0445]

[17] W. Pyka. *Feature Scale Modeling for Etching and Deposition Processes in Semiconductor Manufacturing*. Dissertation, Technische Universität Wien, 2000. http://www.iue.tuwien.ac.at/phd/pyka.

[raupp]

[18] G.B. Raupp, F.A. Shemansky, and T.S. Cale. Kinetics and mechanism of silicon dioxide deposition through thermal pyrolysis of tetraethoxysilane. *J. Vac. Sci. Technol. B*, 10(6):2422–2430, 1992.

[A0496]

[19] G. Schumicki and P. Seegebrecht. *Prozeßtechnologie*. Springer, 1991.

[sethian1994curvature]

[20] J.A. Sethian. Curvature flow and entropy conditions applied to grid generation. *J. Comput. Phys.*, 115(2):440–454, 1994.

[A0739]

[21] J.A. Sethian. *Level Set Methods and Fast Marching Methods*. Cambridge University Press, Cambridge, 1999.

[sethian2001evolution]

[22] J.A. Sethian. Evolution, implementation, and application of level set and fast marching methods for advancing fronts. *J. Comput. Phys.*, 169(2):503–555, 2001.

[smith1990]

[23] D.L. Smith, B. Wacker, S.E. Ready, C.C. Chen, and A.S. Alimonda. Mechanism of SiN_xH_y deposition from NH_3–SiH_4 plasma. *J. Electrochem. Soc.*, 137:614–623, 1990.

[P0287]

[24] K.K.H. Toh, A.R. Neureuther, and E.W. Scheckler. Algorithms for simulation of three-dimensional etching. *IEEE Trans. Computer-Aided Design*, 13(5):616–624, 1994.

List of Figures

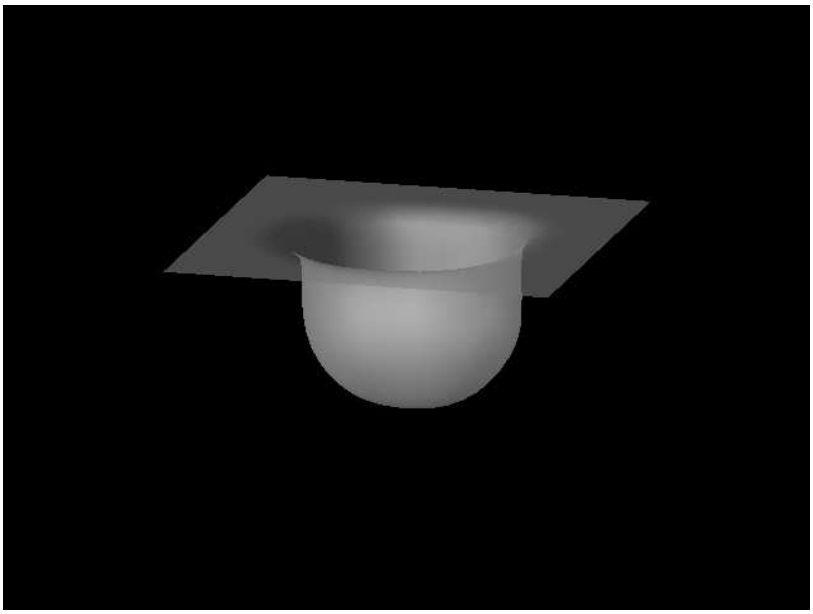

Figure 1: An isotropic etching process.

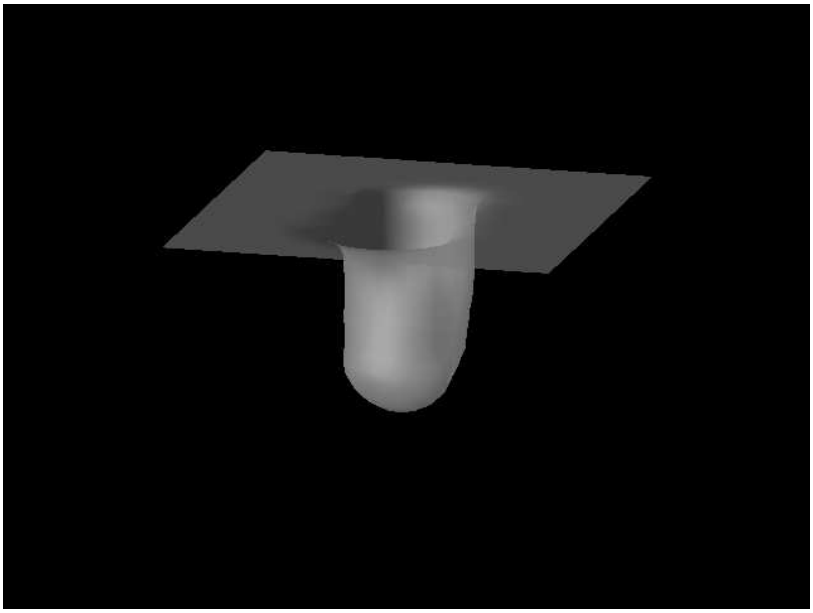

Figure 2: Directional etching.

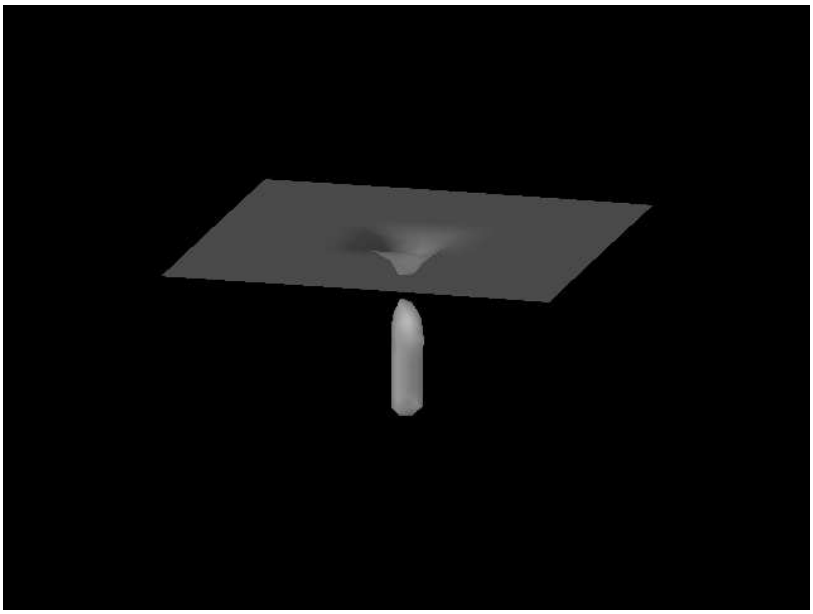

Figure 3: Starting from a rectangular trench, a deposition process results in void formation.

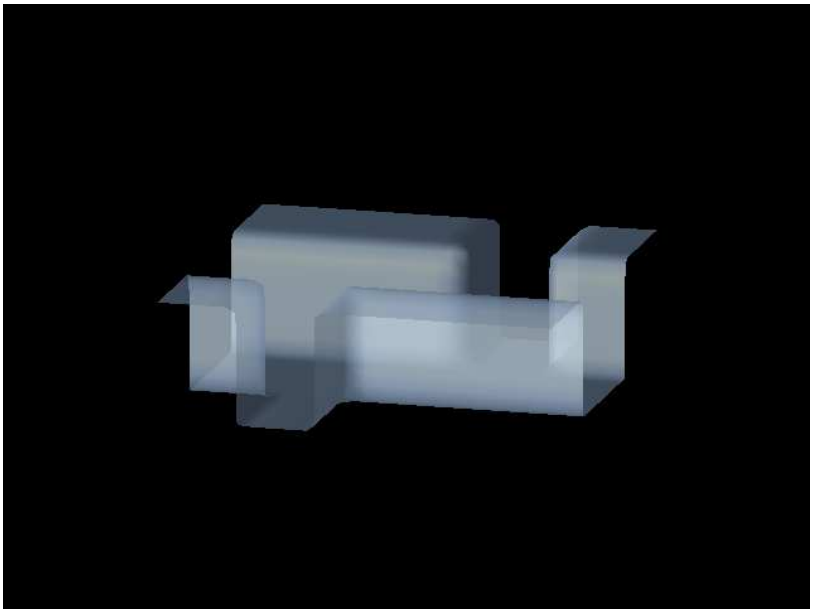

Figure 4: The initial geometry of the H-shaped trenches under consideration.

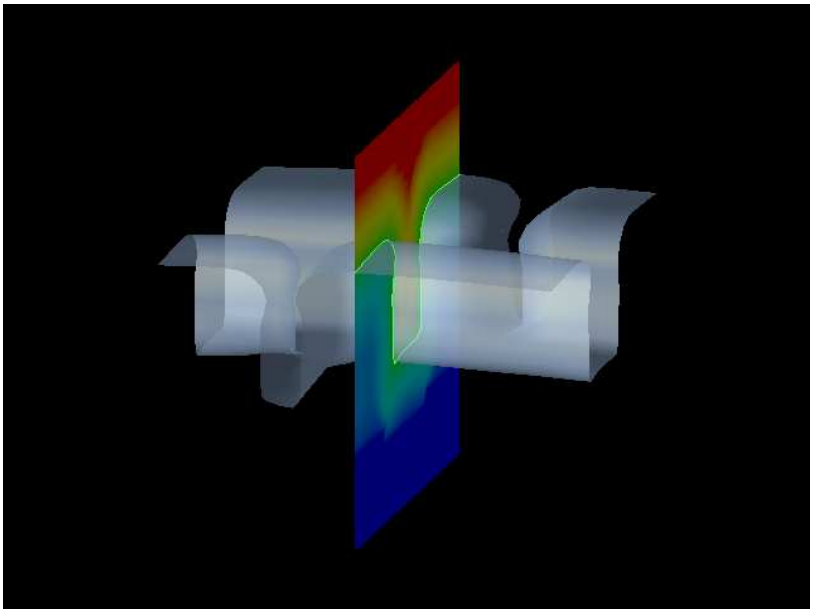

Figure 5: After 35 simulation steps of the deposition of an oxide layer, this surface is obtained using $100 \cdot 100$ point sources. The colored plane indicates the values the level set function.

List of Tables

	Deposition	Etching
Energy	Low	High
Reflection	Luminescent	Specular
Radiosity solver 2D	Direct	Iterative
Radiosity solver 3D	Iterative	Iterative

Table 1: This table shows how the transport of particles is handled by the two- and three-dimensional code.

Grid size	30^3	60^3
Deposition	1.54s	47.4s
Isotropic etching	0.53s	2.77s
Directional etching	0.97s	21.1s

Table 2: This table shows the duration of one time step in three simulations on a 2.8GHz Pentium IV computer.